Canadian Journal of Physics

Research Article

Study of a simplified CoolGal target to support the Phase-0 NEPIR facility

Elizabeth Musacchio-González[a], **Alberto Monetti**[a], **Pierfrancesco Mastinu**[a], **Jeffery Wyss**[b,c], **Luca Silvestrin**[c,d], **and Alberto Campagnolo**[e]

[a]Laboratori Nazionali di Legnaro - INFN, Viale dell'Università 2, 35020 Legnaro, Padova, Italia; [b]Dipartimento di Ingegneria Meccanica e Civile, Università di Cassino and Southern Lazio, Via G. Di Biasio 43, 03043 Cassino, Italia; [c]Istituto Nazionale di Fisica Nucleare, Sezione di Padova, Via Marzolo 8, 35131 Padova, Italia; [d]Dipartimento di Fisica e Astronomia, Università di Padova, Via Marzolo 8, 35131 Padova, Italia; [e]Dipartimento di Ingegneria Industriale, Università di Padova, Via Venezia 1, 35131 Padova, Italia

Corresponding author: **Elizabeth Musacchio-González** (email: musacchio@lnl.infn.it)

Abstract

The NEPIR facility (NEutron and Proton Irradiation), currently in development at the Laboratori Nazionali di Legnaro of the Istituto Nazionale di Fisica Nucleare (LNL-INFN), will serve as the first fast neutron ($E_n > 1$ MeV) irradiation source in Italy specifically designed to support advanced scientific research and industrial applications. Powered by the SPES (Selective Production of Exotic Species) variable-energy proton cyclotron, NEPIR will be implemented in two main phases. Phase-0 will deliver continuous (white spectrum) and pseudo quasi-monoenergetic neutron fields, while Phase-1 will introduce true quasi-monoenergetic neutron beams and an atmospheric-like neutron spectrum. The Phase-0 target system, CoolGal, is based on a thick beryllium target and is intended to evolve into a galinstan-cooled configuration for high-power operation. To simplify initial commissioning, a water-cooled prototype—excluding galinstan—has been developed. This paper presents thermal and structural analysis of the prototype and evaluates its neutron production performance through Monte Carlo simulations. The primary goal is to support an experiment to measure the double-differential neutron yield of the Be(p,n) reaction in the 30–70 MeV range. These results will provide new experimental data to supplement current Japanese Evaluated Nuclear Data Library evaluations and guide the development of advanced neutron sources at NEPIR.

Key words: neutron production, beryllium target, CANS

1. Introduction

Compact accelerator-driven neutron sources (CANS) already play an important role in applications of neutron physics, and their importance will continue to grow. As research nuclear reactors close, CANS provide a cost-effective alternative, supporting communities in need of easy-to-access neutron beams; in addition, their distributed nature allows for broader accessibility, including use as training centers. The growing relevance of CANS is reflected in international networks such as UCANS (Union for Compact Accelerator-driven Neutron Sources) [1] and ELENA (European Low Energy accelerator-based Neutron facilities Association) [2], which coordinate efforts among facilities worldwide.

Within this context, the NEPIR (NEutron and Proton Irradiation) facility is a multidisciplinary project at the Laboratori Nazionali di Legnaro (LNL-INFN) [3]. Powered by the SPES (Selective Production of Exotic Species) variable-energy proton cyclotron, NEPIR will deliver fast neutrons ($E_n > 1$ MeV) in the 30–70 MeV range to support a broad spectrum of applications. These include single event effect testing in electronics, radiation effects on biological systems, shielding verification for space and medical technologies, and the generation of nuclear data for Monte Carlo simulations.

To allow progressive commissioning and enable early experiments, NEPIR will be developed in two main phases. Phase-0 will provide continuous-spectrum (white) neutrons by using a thick, proton-stopping beryllium target. It will also allow the generation of pseudo quasi monoenergetic neutron (PQMN) beams through spectral subtraction techniques using closely spaced proton energies [4]. This approach enables early testing of components and diagnostics, initial neutron yield measurements, and preliminary research in dosimetry, shielding, electronics, and educational training. The target system for this phase, called CoolGal, is designed to handle high power levels using a galinstan-based liquid-metal cooling system to efficiently dissipate heat and stabilize the system thermally.

Phase-1 will significantly expand NEPIR's capabilities by introducing true Quasi Monoenergetic Neutron (QMN) beams using thin lithium or beryllium targets, allowing precise energy selection in the 30–70 MeV range [4]. A dedicated Atmospheric Neutron Emulator (ANEM) target will also be implemented to replicate the energy spectrum of cosmic-

Fig. 1. Cross-section of the simplified CoolGal prototype showing the beryllium target, window, and cooling system.

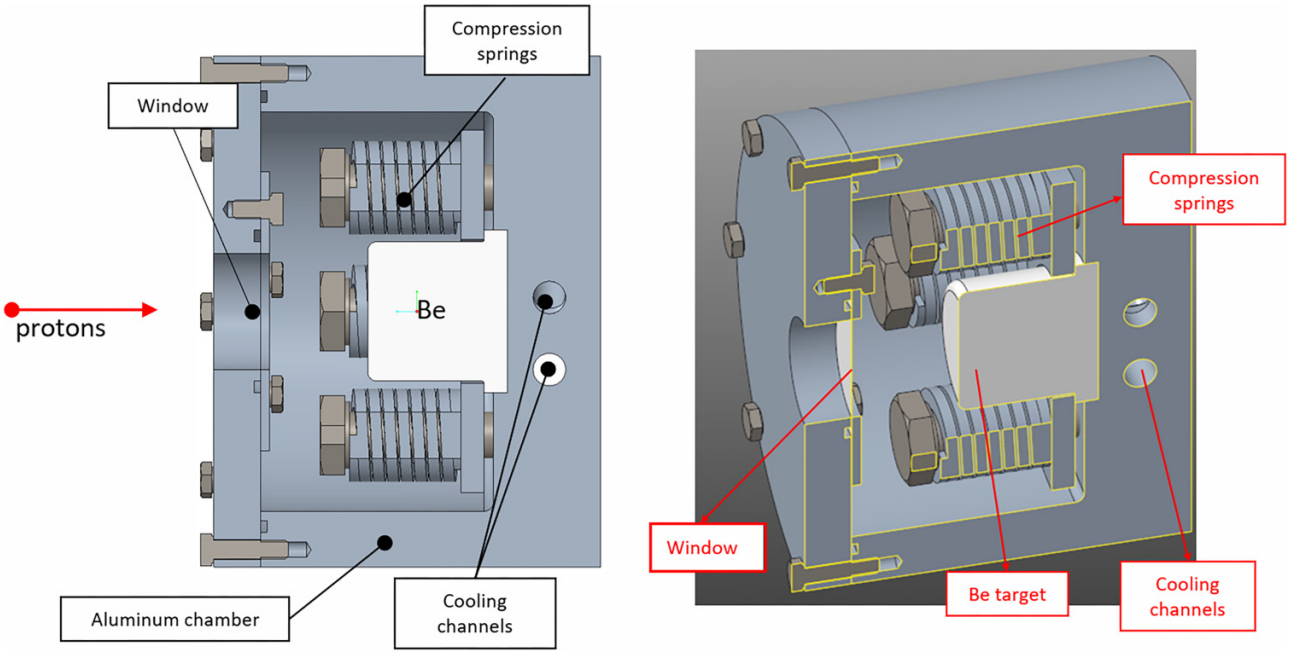

ray-induced atmospheric neutrons within the accessible energy range. This will support research in space electronics, aviation safety, and high-reliability systems. More details of the ANEM target are found in Mastinu et al. [4] and Acosta Urdaneta et al. [5]. These advancements will enable more accurate neutron cross-section measurements, calibration of radiation detectors, and benchmarking of radiation transport codes. The modular and flexible design of NEPIR will allow it to serve a wide user community spanning fundamental research, applied technology, and industrial testing.

A key milestone in Phase-0 is the development of the CoolGal target system, designed to produce continuous energy fast neutron beam via proton-induced reactions on a thick beryllium target. The CoolGal target system consists of a 30 mm beryllium disk, encased in a coated copper or aluminum cladding and submerged in a static galinstan (SnInGa alloy) bath for efficient heat removal and thermal stabilization, making it well suited for high-power target cooling. A thin window, capable of withstanding pressure differences up to 1 atm, separates the liquid metal from the beamline vacuum. The CoolGal target was originally designed for high power dissipation (>1.5 kW); see Mastinu et al. [4] and Alfonso-Barrera et al. [6] for further design details. While the final design will employ a galinstan cooling system, a simplified version has been studied without galinstan to enable earlier testing and reduce system complexity.

This simplified prototype is the focus of the present work. The prototype's development, currently under assembly, aims to validate thermal simulations, evaluate the mechanical performance of the separation window and beryllium target under realistic beam-induced stresses, and assess operational aspects relevant for commissioning. A key objective is to support a proposed experiment at SPES focused on measuring the double-differential neutron yield of the Be(p,n) reaction in the 30–70 MeV proton energy range. Despite the relevance of this reaction for fast neutron production, experimental data at these energies remain limited and are primarily derived from JENDL (Japanese Evaluated Nuclear Data Library) evaluations. New high-precision measurements will help refine neutron source designs and are particularly important for optimizing the final configuration of the ANEM target in NEPIR Phase-1.

The following sections present the prototype's design, simulation results on structural, thermal, and expected neutron spectrum, and implications for future NEPIR development.

2. Design of the simplified CoolGal prototype

A simplified, low-power prototype of the CoolGal target—without galinstan cooling—has been developed for upcoming tests at the SPES cyclotron. The primary objectives are to validate thermal simulations, assess the mechanical performance of the separation window and target assembly under beam conditions, and measure the double-differential neutron yield of the Be(p,n) reaction in the 30–70 MeV range.

Figure 1 shows a section of the prototype; it consists of a thick beryllium block pressed to a water-cooled aluminum vacuum chamber. The vacuum environment is maintained using the thin separation window. While the final CoolGal galinstan-cooled target is being designed, constructed, and tested, the prototype system will provide neutron beams to support academic and industrial research. The following sections provide further details on this prototype's components and key characteristics.

2.1. Separation window

The separation window maintains vacuum integrity while allowing proton beam passage and isolating the target environment from the accelerator beamline. Materials were selected based on thermal conductivity, radiation resistance, mechanical strength, activation levels, and cost. Four candidates were considered: aluminum alloy 6061, titanium alloys Grade 5 and Grade 9, and Havar.

Simulations determined the optimal thickness and thermal response of each material under different beam conditions using ANSYS [7] for Finite Element Analysis (FEA). FLUKA Monte Carlo simulation code [8, 9] was used for residual activity and radiation dose at 1 meter after 100 days of irradiation. Proton energies from 30 to 70 MeV and currents of 1 and 10 μA were studied. Simulations, detailed in Section 3.1, guided material selection.

2.2. Beryllium target

The target consists of a simple beryllium cylinder with a specially machined base to allow it to be pressed against the bottom of the chamber (see Fig. 1). The beryllium cylinder is mechanically secured to optimize thermal contact with the cooling surface while avoiding overstress in the support structure.

Once the geometry was defined, thermal analysis became essential, particularly for the beryllium target. FEA were conducted using ANSYS software [7] to simulate the thermal behavior of the target under beam exposure. Proton beam energies of 30–70 MeV at currents of 1 and 10 μA were analyzed. Critical scenarios were also evaluated, including the initiation of a crack in the beryllium target. The results of these analyses are presented in Section 3.2.

The beam is fully stopped within the material for 70 MeV protons incident on a 30 mm thick beryllium target. This results in a greater temperature increase compared to cases where the beam exits the beryllium, posing risks to the material's integrity due to potential blistering and flaking. An alternative design with a 26 mm beryllium target thickness was considered to mitigate these risks, allowing the beam to stop in the aluminum chamber rather than within the beryllium itself. The beryllium piece for this project will not be manufactured in laboratory workshops but will be procured from external companies specializing in beryllium processing.

2.3. Cooling system

The most commonly used cooling system, including the one in our laboratories, consists of channels running through the chamber's thickness. A liquid—typically water—flows through these channels, efficiently dissipating heat from the target. The cooling system was designed to dissipate 700 W of power with a water flow rate of approximately 200 l/h, resulting in a maximum temperature increase of 55 °C at the point of contact with the beryllium target.

Although water was initially considered the cooling fluid, its circulation within the irradiated chamber posed management challenges. To address this, an alternative cooling approach using compressed air available at the facility was explored. Cooling system performance is further discussed in Section 3.3.

Table 1. Minimum thickness of the separation window and maximum temperature in the window for 1 μA and 35 MeV (worst-case scenario).

Material	Minimum thickness (μm)	Maximum temperature (°C)
Ti-Gr5	25	110
Ti-Gr9	30	105
Al-6061	90	40
Havar	50	120

3. Results and discussion

3.1. Separation window

The material's elastic–plastic behavior was considered when determining the optimal thickness to mitigate stress concentrations at the clamping point [10]. Unlike the bulk beryllium target, the most critical scenario for the window occurs with a 35 MeV proton beam, which results in higher temperatures than the 70 MeV beam due to increased stopping power.

FEA identified the center of the window as the hottest region, with aluminum demonstrating superior thermal performance despite requiring greater thickness. In contrast, Havar reached higher temperatures and residual dose levels, raising safety and activation concerns. Table 1 summarizes the minimum required thicknesses and peak temperatures. For further details on studies related to the thermal analysis of the window, see Dattilo R. [10].

Using the FLUKA Monte Carlo simulation code [8, 9], the radiation dose absorbed over time due to the residual radioactivity of the window was evaluated, considering an irradiation period of 100 days with a beam energy of 35 MeV and a current of 1 μA. A mannequin was positioned 1 meter from the window to simulate the received dose. The activity of potential materials for the CoolGal window was also simulated under the same conditions. Figure 2 compares (left) the dose received by the mannequin for different materials and (right) the activity of these materials over time.

FLUKA simulations showed aluminum has the lowest activity during the first 200 days post-irradiation, making it advantageous for operations with short cooldown periods. Titanium alloys offer intermediate activation but greater strength, while Havar's slow decay and poor thermal efficiency limit its suitability. These results indicate that aluminum offers the best thermal performance, while titanium alloys present a trade-off between strength and thermal efficiency. Havar, though historically used, appears suboptimal due to high temperature and residual activity. Complementary experimental tests were conducted to measure the breakout pressure of each window material. Based on both the simulation outcomes and experimental measurements, the final selection of a 100 μm Al window for the prototype was due to its thermal efficiency and lower activation.

Fig. 2. (Left) Dose received by a mannequin at 1 m. (Right) Activity of the different materials over time. In both simulations, an irradiation period of 100 days with a beam energy of 35 MeV and 1 μA current was considered.

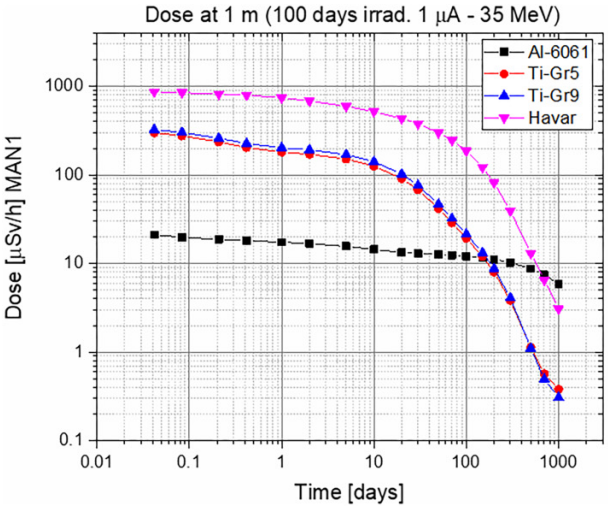

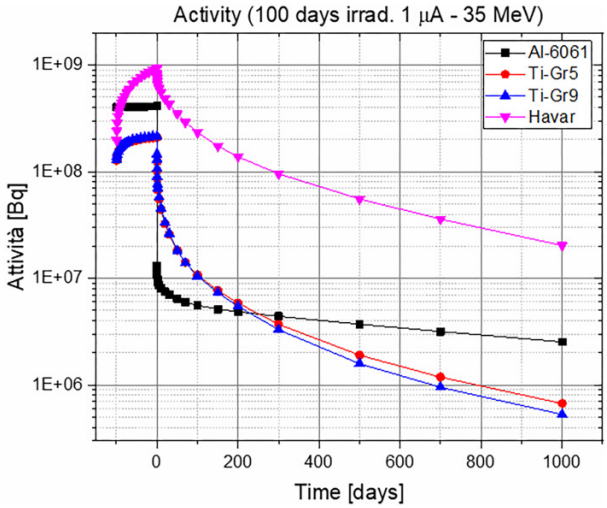

Fig. 3. Thermal field within the target cross-section for 70 MeV protons with 1 μA (70 W).

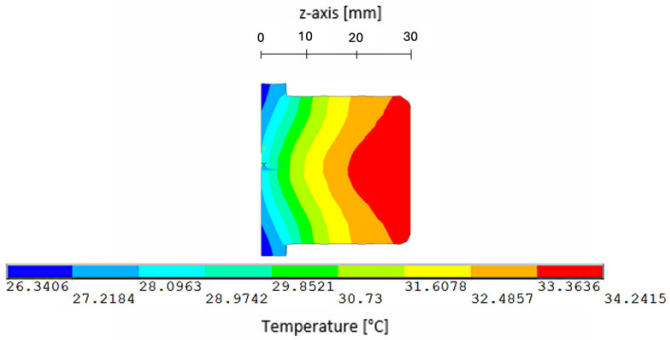

Fig. 4. Temperature distribution along the target axis for different power depositions.

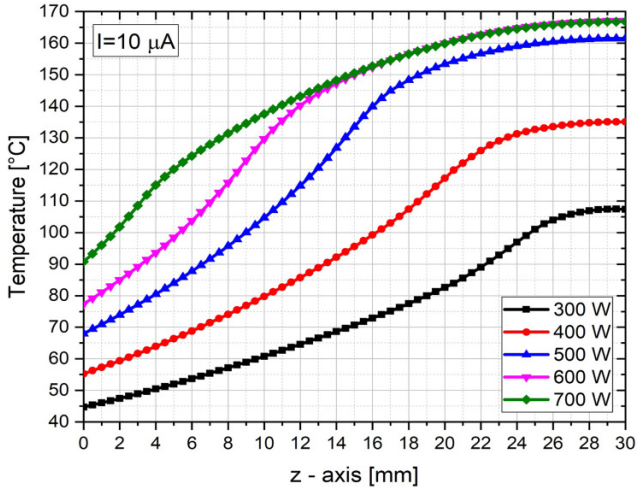

3.2. Beryllium target

Initial simulations were performed with a proton beam current of 1 μA, yielding power deposition values ranging from 35 to 70 W. The power deposition distribution was computed using FLUKA [8, 9], assuming a Gaussian proton beam profile with a 5 mm root mean square deviation, and subsequently imported into ANSYS [7] for thermal analysis.

The thermal distribution within the target was analyzed for each power setting, with the most critical scenario occurring at 70 W. Figure 3 illustrates the temperature field in a section of the target for this case. The results indicate that the maximum temperature, 35 °C, occurs on the upper surface of the target—the region farthest from the cooling channels located at the base. Subsequent simulations were conducted with a beam current of 10 μA. The results, shown in Fig. 4, indicate that the top surface of the beryllium is the most thermally stressed, especially at beam powers exceeding 600 W. A maximum temperature of 168 °C was observed for 700 W power deposition. The key degradation phenomena for beryllium under proton impact include sputtering [11, 12], erosion caused by high temperatures [13], material loss due to target oxidation [14], and melting. Despite this, temperatures remain below thresholds for significant sputtering or melting. At 10 μA (a flux of about 10^{14} p/cm^2/s), the beryllium atom loss rate of 10^{11} atoms/cm^2 is considered insignificant.

After conducting simulations under nominal conditions, the system's behavior was analyzed in the presence of disturbances that disrupt its equilibrium, such as the initiation of a crack within the target. Simulations of lateral cracks at the Bragg peak depth revealed increased local temperatures and spatial asymmetries, with surface temperatures reaching 240 °C for the worst case. The inclusion of thermocouples is thus critical to detect such anomalies in real time. To address this, modifications were made to the latest model of the target: holes were introduced for the insertion of thermocouples. Thermocouples were embedded at three axial positions to monitor temperature gradients near the Bragg peak. Thermal simulations validated a 26 mm thick beryllium target de-

Fig. 5. Design of the cooling channels inside the aluminum chamber, to dissipate 700 W of the target.

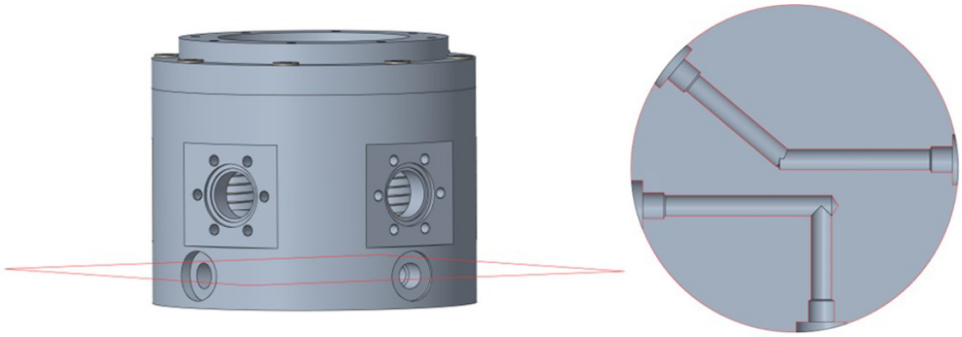

sign and confirmed the importance of integrated thermocouples for detecting early-stage thermal anomalies, including those caused by internal cracking.

3.3. Cooling system

The cooling channel dimensions were determined through an iterative design process that accounted for the required heat dissipation (700 W), the cooling system's maximum flow rate (200 L/h), water velocity, and the expected heat transfer coefficient. Based on these parameters, a channel with a 7 mm diameter and 214 mm length was selected, yielding an estimated forced convection coefficient of approximately 8 kW/m^2 ·°C. The final channel geometry is illustrated in Fig. 5. Thermal modeling of the aluminum chamber showed a symmetric temperature distribution with a peak of 76 °C, validating the channel geometry and flow rate assumptions.

Assuming the same temperature increase of 55°C for the chamber, various cooling options were explored in the absence of water. The study considered using natural convection or compressed air as coolants. Natural convection alone can efficiently dissipate up to 20 W of power. However, with compressed air, it is possible to dissipate between 70 W and 150 W, depending on the available airflow rate. For low- and mid-power operation, alternative cooling with compressed air is assessed. Natural convection suffices for proton currents below 0.3 μA; compressed air is adequate up to 2 μA, beyond which water cooling is required. For high-power dissipation (>1.5 kW), a target with galinstan coolant is mandatory.

3.4. Neutron energy spectra

An alternative design featuring a 26 mm thick target was explored to reduce the risk of blistering and excessive temperature rise, at least for 70 MeV protons, the highest beam energy at SPES. In this design, the beam is stopped in the aluminum chamber rather than the beryllium. Simulations of the expected neutron spectrum emitted from the simplified CoolGal prototype target (Section 2) were performed with the MCNPX Monte Carlo code [15], considering the two beryllium thicknesses (originally 30 mm and the new 26 mm). Reducing target thickness from 30 mm to 26 mm had minimal effect on the neutron yield, except for a minor 7% reduction below 3 MeV. Given that the intended application focuses on fast neutrons, the minor reduction in low-energy neutron yield is considered acceptable, and the target thickness was therefore fixed at 26 mm.

Fig. 6. MCNPX simulations of the expected neutron energy spectra (in the forward direction, with a 3° semi-angle, at 1 m) with a 26 mm thick beryllium target and 0.1 mm aluminum window.

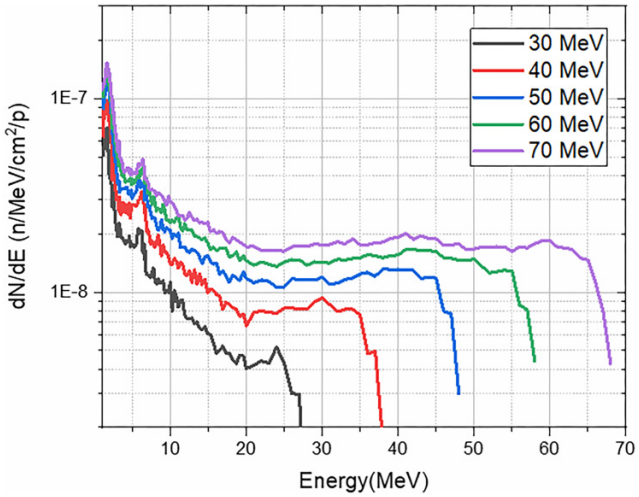

Figure 6 shows the simulated neutron energy spectra, in the forward direction (3° semi-angle), at 1 m, with the complete prototype target (Fig. 1 but 26 mm beryllium). In the figure, the simulations for different proton energies are shown. The integral fast ($E_n > 1$ MeV) neutron flux for 70 MeV protons is 10^6 n/cm^2/s at 1 m.

PQMN beams can be effectively produced by energy subtraction methods [4], offering flexible spectrum shaping capabilities without dedicated QMN targets. Figure 7 shows an example of such a PQMN spectrum (blue) obtained by the subtraction of the neutron energy spectrum generated by 67 MeV protons (black) from the 70 MeV spectrum (red), for a proton current of 1 μA at a downstream point distant of 1 m.

Experimental validation of these simulations will provide critical input for the final CoolGal and NEPIR Phase-0 design. Testing the simplified CoolGal prototype without Galinstan is being considered at the SPES proton cyclotron. A key goal will be to measure the double-differential neutron yield of the Be(p,n) reaction, a crucial process for copious production

Fig. 7. An effective pseudo quasi mono-energetic neutron (PQMN) spectrum (blue) obtained by subtraction: the neutron energy spectrum generated by 67 MeV protons (black) is subtracted from the 70 MeV spectrum (red).

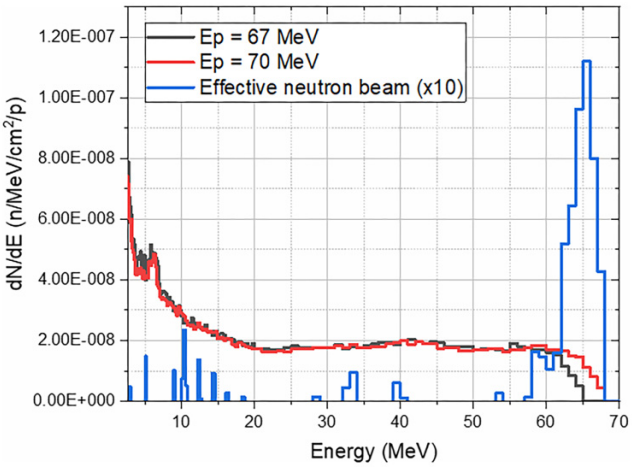

of fast neutrons. Two independent methods will be employed to measure the neutron energy spectrum and validate simulation results: the standard stack-activation foil technique and a plastic scintillator-based fast neutron detector [16]. The latter was developed at the University of Cape Town (UCT) and characterized at several fast and high-energy neutron facilities, including the UCT and iThemba LABS. These measurements will be conducted in collaboration with iThemba LABS.

In addition, two other detectors are under development for this measurement: a proton recoil telescope following the configuration of Yoshiaki Shikaze et al. [17] and a novel honeycomb-shaped scintillator detector. Both systems rely on the well-characterized (n,p) reaction cross section. Calibration and characterization of these detectors must be completed prior to their use; if successful, they will also be included in the experimental campaign.

4. Conclusions

This work presents the design and analysis of a simplified CoolGal prototype developed for NEPIR Phase-0. The target assembly, excluding galinstan cooling, was engineered to validate thermal simulations, assess mechanical performance under beam-induced stresses, and support early commissioning at the SPES cyclotron. A central objective is the experimental measurement of the double-differential neutron yield of the Be(p,n) reaction in the 30–70 MeV proton energy range, for which existing data remain limited and largely based on evaluations.

Thermal and radiation analyses guided critical design decisions, including the selection of a 100 μm aluminum separation window and a 26 mm thick beryllium target, both optimized for heat dissipation and operational safety. Cooling strategies were evaluated for varying beam powers, confirming that air convection is viable at low currents, while water cooling is required beyond 2 μA.

Prototype testing will not only validate the simulation framework, but also guide the final design of the CoolGal target. These developments are essential for the phased construction of a dedicated NEPIR beamline and bunker at the SPES facility. Even with this simple prototype target, the infrastructure will support the timely delivery of fast neutron beams to a broad spectrum of users from academia and industry.

Article information

History dates
Received: 31 March 2025
Accepted: 28 August 2025
Accepted manuscript online: 9 September 2025
Version of record online: 29 October 2025

Notes
This paper is one of a selection of papers from the 11th International Meeting of the Union for Compact Accelerator-driven Neutron Sources.

Data availability
Data generated or analyzed during this study are available from the corresponding author upon reasonable request.

Author information

Author ORCIDs
Elizabeth Musacchio-González https://orcid.org/0000-0002-4070-9204

Author contributions
Conceptualization: EMG, AM, PM, JW, LS, AC
Data curation: EMG, AM, PM
Formal analysis: EMG, AM
Funding acquisition: AM, PM, JW, AC
Investigation: EMG, AM, LS
Methodology: EMG, AM, PM, JW, LS, AC
Project administration: AM, JW, AC
Resources: EMG, AM
Software: EMG, AM
Supervision: EMG, AM, AC
Validation: EMG, AM, PM, JW, AC
Visualization: EMG, AM, JW
Writing – original draft: EMG
Writing – review & editing: EMG, AM, PM, JW, LS, AC

Competing interests
The authors declare there are no competing interests.

Funding information
We acknowledge the financial support provided under the National Recovery and Resilience Plan (NRRP), Mission 4, Component 2, Investment 1.1, call for tender No. 104, pub-

lished on 2 February 2022, by the Italian Ministry of University and Research (MUR), funded by the European Union NextGenerationEU Project, “CoolGal: A Liquid Metal-Cooled Beryllium Target for a Proton-Induced Neutron Production”–Code MUR 2022JCS2CN_002–CUP C53D23001500001–Grant Assignment Decree No. 974, adopted on 30/06/2023 by the Italian Ministry of University and Research (MUR).

References

1. Union for compact accelerator-driven neutron sources (UCANS). Available from https://www.ucans.org.
2. European low energy accelerator-based neutron facilities association (ELENA). Available from https://elena-neutron.iff.kfa-juelich.de.
3. Legnaro National Laboratories (LNL). Available from https://www.lnl.infn.it/index.php/en/.
4. P. Mastinu, D. Bisello, R.A. Barrera, I. Porras, G. Prete, L. Silvestrin, and J. Wyss. J. Neutron Res. **22**, 233 (2020). doi:10.3233/JNR-200156.
5. G.C. Acosta Urdaneta, D. Bisello, J. Esposito, P. Mastinu, G. Prete, L. Silvestrin, and J. Wyss. IL Nuovo Cimento C, (2015). doi:10.1393/ncc/i2015-15184-0.
6. R. Alfonso Barrera, D. Bisello, J. Esposito, P. Mastinu, G. Prete, L. Silvestrin, and J. Wyss. EPJ Web Conf. **231**, (2020). doi:10.1051/epjconf/202023103002.
7. Ansys® Academic Research Mechanical, Release 18.2. Available from https://www.ansys.com.
8. T.T. Böhlen, F. Cerutti, M.P.W. Chin, A. Fassò, A. Ferrari, P.G. Ortega, A. Mairani, P.R. Sala, G. Smirnov, and V. Vlachoudis. Nucl. Data Sheets, **120**, 211 (2014). doi:10.1016/j.nds.2014.07.049.
9. A. Ferrari, P.R. Sala, A. Fassò, and J. Ranft. CERN-2005-10, INFN/TC05/11, SLAC-R-773. (2005). Available from http://www.fluka.org/fluka.php.
10. D. Roberta. Eng. Proc. **85**, (2024). doi:10.3390/engproc2025085028.
11. N. Matsunami, Y. Yamamura, Y. Itikawa, N. Itoh, Y. Kazumata, S. Miyagawa, K. Morita, R. Shimizu, and H. Tawara. At. Data Nucl. Data Tables, **31**, 1 (1984). doi:10.1016/0092-640X(84)90016-0.
12. E. Torresin. Progettazione meccanica, simulazione e test sperimentali di un target per la produzione di fasci di neutroni per il progetto CoolGal. PhD thesis, University di Padua, 2024. Available from thesis.unipd.it.
13. R.P. Doerner, M.J. Baldwin, S.I. Krasheninnikov, and K. Schmid. J. Nucl. Mater. **337–339**, 877 (2005). doi:10.1016/j.jnucmat.2004.09.025.
14. E.A. Gulbransen, and F.A. Kenneth. J. Nucl. Mater. **97**, 383 (1950). doi:10.1149/1.2777899.
15. D.B. Pelowitz. LA-CP-11-00438(2011).
16. A. Buffler, T. Hutton, E. Jarvie, and R. Babut. Rad. Phys. Chem. **220**, (2024). doi:10.1016/j.radphyschem.2024.111698.
17. J.S.G. Yoshiaki Shikaze, Y. Tanimura, and M. Tsutsumi, Nucl. Instr. Methods Phys. Res. A, **615**, 211 (2010). doi:10.1016/j.nima.2010.01.032.